OPTIMUM LATTICE ARRANGEMENT DEVELOPED FROM A RIGOROUS ANALYTICAL BASIS*

John DeYoung
Vought Corporation Hampton Technical Center

SUMMARY

The spanwise vortex-lattice arrangement is mathematically established by lattice solutions of the slender wing which are shown to be analogous to the chordwise vortex-lattice thin wing solution. Solutions for any N number of panels to infinity are obtained. With the optimum lattice for any N value the slender wing theory lift and induced drag and thin wing theory lift and moment are predicted exactly. For $N \to \infty$, slender wing elliptic spanwise loading and thin wing cotangent chordwise loading are predicted, which proves there is mathematical convergence of the vortex-lattice method to the exact answer. Based on this $A \to 0$ and an $A \to \infty$ planform spanwise lattice arrangements, an A-vortex-lattice spanwise system is developed for arbitrary aspect ratio. This A-lattice has the optimum characteristic of predicting lift accurately for any N value.

INTRODUCTION

Growth of computer facilities has given the engineer a powerful tool for obtaining solutions to generalized problems. This is possible because with numerical or finite-difference methods the equations of a problem can be simplified readily to computer language. Vortex-lattice methods have been developed extensively for steady and unsteady pressure prediction and for planar and nonplanar configurations. Examples of some of the work and investigations in the vortex-lattice method and aspects and applications of this method are reported in references 1 through 20. A brief description of the typical vortex lattice is that the surfaces are divided in the spanwise and chordwise directions into panels which cover the surface with a lattice. The sides of the panels are parallel to the freestream and the chordwise panel boundaries follow the surface contour. The 1/4 chord line of each panel contains a bound or load vortex while the trailing vortices are at the sides of the panel. The boundary condition of no flow through the surface is fulfilled on every panel at one point located at the lateral center of the 3/4 chord line of the panel. These panels are distributed in a uniform, and thus geometrically simplest mesh, referred to as a planform lattice. However, in

*Preparation of this paper was supported principally under NASA Langley Contract No. NAS1-13500.

1966 an application of the lattice method of reference 5 to a swept wing showed that the chord loading in the panel bordering the wing leading edge was too low, the spanwise loading near the wing tip was too high for engineering acceptability, and the net lift slightly too large. This was with 100 panels on the semispan, 10 chordwise times 10 spanwise. Investigation of a lattice mathematical model was made at that time of the chordwise panel distribution and later reported in reference 20. The results of this work showed that the loading at the leading edge panel needs a factor of about 1.128 which improved the loading value in that panel. However, the too high wing tip loading and lift was not explained. In early 1972 a mathematically rigorous spanwise vortex-lattice analysis was developed based on slender wing theory (part of ref. 19). This was mathematically analogous to the earlier chordwise solution but more complicated. This spanwise lattice arrangement is characterized by a 1/4 - 3/4 rule which locates the trailing vortices inboard 1/4 of the planform panel span and the no flow through points inboard 3/4 of planform panel span from the planform panel outboard edges. This inboard shift of the lattice leads to solutions with less loading near the wing tip and less lift, which improves the loading in the above example. This example supports the observation that accuracy depends on the position of the panels in the lattice as well as density of panels.

The objectives of the present study are to correlate and extend the work of references 19 and 20, to investigate the effect of three-dimensional planform on lattice arrangement, and to formulate a generalized vortex-lattice arrangement and method for three dimensional wings.

SYMBOLS

A	aspect ratio
A_e	swept panel aspect ratio [eq. (52)]
b, c	wing span, wing chord
C_L, C_{L_α}	lift coefficient, lift-curve slope
C_{D_i}	induced drag coefficient
c_ℓ, c_{ℓ_α}	section lift coefficient, section lift-curve slope
$c_{m_{\alpha_{LE}}}$	section pitching moment coefficient due to angle of attack
$e_{N_C n_C}$	parameter of chordwise loading [eq. (38)]
$f_{N_C n_C}$	chordwise loading factor [eq. (41) and table 5]
G	spanwise loading coefficient or dimensionless circulation [eq. (1)]
g_{Nn}	parameter of spanwise incremental circulation [eq. (7)]

h_{Nn} spanwise loading gradient factor [eq. (19) and table 2]

i_{Nn} spanwise loading factor [eq. (22) and table 3]

N, N_C integer number of panels on wing semispan, and wing chord respectively

n,m integers denoting spanwise position of vortex, and downwash point

n_C, m_C integers denoting chordwise position of vortex, and downwash point

V free stream velocity

α angle of attack

Γ circulation, also Gamma function

η lateral coordinate per wing semispan

$\Lambda_{1/2}$ sweep angle at 50% chord line

ξ longitudinal coordinate per wing section chord

Subscripts:

v vortex

w downwash point

LE leading edge

SLENDER WING OPTIMUM VORTEX LATTICE

Physical Similarity of Trailing Vortex Sheet Flow with Chordwise Thin Wing Theory Flow

The objective of this study is to do a rigorous analytical derivation to determine the optimum spanwise distribution of panels analogous to the analysis done in reference 20 for the optimum chordwise distribution of panels. Optimum here defines the lattice which best duplicates exact solutions. A physical similarity does exist between the vorticity distribution of the chordwise loading with the trailing vortex sheet from a finite span wing. This can be seen graphically in figure 1 where thin airfoil theory chord-load vorticity is compared with the trailing vorticity which is predicted by slender wing theory (refs. 21 and 22). It has often been noted that the mathematics of thin wing and slender wing theories have a striking similarity.

From figure 1, it is noted that a similarity of vorticity is obtained when the wing tip at $\eta = 1$ correlates with the wing leading edge, and the

midspan point at $\eta = 0$ correlates with the wing trailing edge. Since this correlation makes the flow fields analogous, it follows that the optimum spanwise panel distribution is analogous to the optimum chordwise panel distribution given in reference 20. This is subject to the condition that the distribution start at the wing tip and proceed inboard. Applying this condition and using these distribution conditions, the spanwise panel distribution becomes that shown in figure 2. The determination of an optimum chordwise panel distribution is made by two-dimensionalizing the problem to planar flow and thus the spanwise extent of the panel is infinite. The optimum chordwise panel distribution is that which yields thin wing solutions which most accurately duplicate the results of exact thin airfoil theory. In the present work, the determination of an optimum spanwise panel distribution will be made by two-dimensionalizing the problem to cross-sectional flow and thus the chordwise extent of the panel is infinite. The optimum $A \to 0$ spanwise panel distribution is that which yields solution which most accurately duplicates the results of slender wing theory.

The objective of the present paper is to apply the analytical methodology of reference 20 to determine the optimum spanwise panel distribution. This distribution should result in an exact prediction of total lift for any number of spanwise panels and provide spanwise loading factors. The chordwise panel distribution analysis is correlated with thin airfoil theory for the determination of optimal accuracy. In an analogous procedure the spanwise panel distribution analysis here will be correlated with slender wing theory for the determination of optimal accuracy.

Formulation of Spanwise Lattice Matrix and Solution to Infinity which Satisfy All Boundary Points

Slender wing theory equations for additional loading (ref. 22) are

$$C_{L_\alpha} = \frac{\pi A}{2}; \quad G_\alpha(\eta) = (1 - \eta^2)^{1/2}; \quad \frac{dG_\alpha(\eta)}{d\eta} = \frac{-\eta}{(1 - \eta^2)^{1/2}} \tag{1}$$

where $G_\alpha(\eta) = \frac{\Gamma(\eta)}{bV\alpha} = \frac{c_\ell c}{2b\alpha}$

Also presented in reference 22 are solutions for flap, ailerons, and all spanwise loadings, which can be used to evaluate lattice accuracy when a problem involves these types of loadings.

By Biot-Savart law, the downwash at η_{wm} due to an infinite extent vortex at η_{vn} is (see fig. 2)

$$w_{mn} = \frac{\Delta\Gamma_n/b}{\pi(\eta_{vn} - \eta_{wm})} \tag{2}$$

with vortices located at

$$n_{vn} = \pm \frac{n - 1/4}{N} \tag{3}$$

boundary condition points at

$$n_{wm} = \pm \frac{m - 3/4}{N} \tag{4}$$

with equations (3) and (4) the downwash angle at n_{wm} is

$$\frac{\alpha_m}{\alpha} = \sum_{n=1}^{N} \left(\frac{1}{n_{vn} - n_{wm}} + \frac{1}{n_{vn} + n_{wm}}\right) \frac{g_{Nn}}{3N} \tag{5}$$

with equations (3), (4), and (5) for additional loading ($\alpha_m=\alpha$), equation (5) becomes

$$1 = \sum_{n=1}^{N} \frac{2}{3} \left(\frac{1}{2n - 2m + 1} + \frac{1}{2n + 2m - 2}\right) g_{Nn};\ m = 1, 2, \ldots N \tag{6}$$

where

$$g_{Nn} = \frac{3N\Delta\Gamma_{Nn}}{\pi bV\alpha} = \frac{3}{\pi} N\Delta G_{\alpha_{Nn}} \tag{7}$$

Generalized Inversion of g_{Nn} Equations

Equation (6) represents N unknowns, g_{Nn}, and N Equations. An inversion of equation (6) means a linear simultaneous solution of N equations. Solutions for N = 1, 2, . . . can be obtained readily for small N and from the resulted series formed of g_{Nn}, the general solution can be determined by induction. For N = 1, the solution is

$$g_{11} = 1$$

For N = 2, the linear simultaneous solution of two equations is

$$\begin{aligned} 1 &= g_{11} + \frac{7}{18} g_{22}; \qquad \text{then,} \qquad g_{21} = \frac{2}{5} \\ 1 &= -\frac{1}{2} g_{21} + \frac{7}{9} g_{22} \qquad\qquad\quad g_{22} = \frac{54}{35} \end{aligned} \tag{8}$$

These solutions are done for higher values of N until a sequence is formed. This sequence is presented in table 1. Examination of the 1st column in table 1 shows the sequence follows the general term of

for n = 1:

$$g_{N1} = \frac{3N(2N-3)_{odd}!}{(2N+1)_{odd}!} \tag{9}$$

In the second column, ratios of g_{N2}/g_{NL} gives the sequence

N = 2 3 4 5 6

$$\frac{g_{N2}}{g_{N1}} = \frac{3^2x3}{1x7} \quad \frac{3^2x8}{3x9} \quad \frac{3^2x15}{5x11} \quad \frac{3^2x24}{7x13} \quad \frac{3^2x35}{9x15}$$

This shows the general term as [and using g_{N1} from eq. (9)]

for n = 2:

$$g_{N2} = \frac{3^2(N^2-1)\,g_{N1}}{(2N+3)(2N-3)} = \frac{3x3^2(N+1)(N-1)(N)(2N-5)_{odd}!}{(2N+3)_{odd}!} \tag{10}$$

Similarly, ratios of g_{N3}/g_{N2} give the sequence

N = 3 4 5 6

$$\frac{g_{N3}}{g_{N2}} = \frac{5^2x5}{11x4} \quad \frac{5^2x12}{3x13x4} \quad \frac{5^2x21}{5x15x4} \quad \frac{5^2x32}{7x17x4}$$

This shows the general term as [using g_{N2} from eq. (10)]

for n = 3:

$$g_{N3} = \frac{5^2(N^2-2^2)g_{N2}}{2^2(2N-5)(2N+5)} = \frac{3x3^2x5^2(N+2)(N+1)(N)(N-1)(N-2)(2N-7)_{odd}!}{2^2(2N+5)_{odd}!} \tag{11}$$

These sequences of g_{N1}, g_{N2}, and g_{N3} show that

$$g_{N4} = \frac{7^2(N^2-3^2)g_{N3}}{3^2(2N-7)(2N+7)}$$

$$= \frac{3x3^2x5^2x7^2(N+3)(N+2)(N+1)(N)(N-1)(N-2)(N-3)(2N-9)_{odd}!}{3^2x2^2(2N+7)_{odd}!} \tag{12}$$

Then in general the recurrence is [from first equalities of eqs. (10), (11), and (12)]

$$g_{Nn} = \left(\frac{n-1/2}{n-1}\right)^2 \frac{N^2-(n-1)^2}{N^2-(n-1/2)^2}\, g_{N_{n-1}} \tag{13}$$

The general term for net values of g_{Nn} is [from second equalities of eqs. (10), (11), and (12)]

$$g_{Nn} = \frac{3(N+n-1)![(2n-1)_{odd!}]^2\ (2N-2n-1)_{odd!}}{(n-1)![(n-1)!]^2\ (2N+2n-1)_{odd!}} \tag{14}$$

Equation (14) is an exact mathematical inversion of the matri. type represented in equation (6). The equation (14) solution is exact for a' interger value of N, including N equal to infinity.

The odd factorial $(2n-1)_{odd!}$ can be converted to direct factorials by the relation

$$(2n-1)! = (2n-1)_{odd}!\ (2n-2)_{ev}!$$

where $(2n-2)_{ev}! = (2n-2)\ (2n-4)\ (2n-6)\ \ldots\ . = 2^{n-1}(n-1)(n-\ )(n-3)$

$\ldots\ . = 2^{n-1}\ (n-1)!$

then $\quad (2n-1)_{odd}! = (2n-1)!/2^{n-1}(n-1)! \tag{15}$

Using equation (15) in equation (14), then g_{Nn} in terms of conventional factorials is

$$g_{Nn} = \frac{3n^2(2N-2n)!}{(N+n)(2N+2n)!}\left[\frac{(2n)!(N+n)!}{(n!)^2(N-n)!}\right]^2 \tag{16}$$

Factorials suggest Gamma functions. Extensive relations of Gamma functions and tables are presented in reference 23. In terms of Gamma functions equation (16) becomes

$$g_{Nn} = \frac{3n^2\ \Gamma(N-n+1/2)\ \Gamma(N+n+1)}{\pi(N+n)\ \Gamma(N-n+1)\ \Gamma(N+n+1/2)}\left[\frac{\Gamma(n+1/2)}{\Gamma(n+1)}\right]^2 \tag{17}$$

The g_{Nn} function is thus expressed in three forms given by equations (14), (16), and (17) respectively.

Gradient of Spanwise Loading

The spanwise loading gradient is [using eqs. (3) and (7)]

then $\quad G_\alpha{}'(\eta_{vn}) = -\frac{\pi}{3}\, g_{Nn} \tag{18}$

where g_{Nn} is given in equation (16). The spanwise position, η_{vn}, is given by equation (3). Comparable slender wing theory values of $G_\alpha'(\eta_{vn})$ are obtained by replacing η by η_{vn} in the gradient function given in equation (1). Comparison of equation (18) with the slender wing theory value of loading gradient shows that the lattice-method loading gradient requires a factor. This factor can be formulated accurately by this slender wing solution.

The loading gradient factor is defined as

$$h_{Nn} = \frac{G_\alpha'(\eta_{vn})\ \text{slender wing theory}}{G_\alpha'(\eta_{vn})} \tag{19}$$

Numerical values of h_{Nn} computed from equations (19) and (18) are presented in table 2. These factors are very near unity except at the wing tip region. Included are values for $N \to \infty$ determined in a following section.

Spanwise Loading

With the vortex position set by equation (3) the ΔG_{Nn} extends from $\eta_{vn} = (n - 1/4)/N$ to $(n - 1 - 1/4)/N$. The middle of this segment is at $\eta_n = (n - 3/4)/N$, that is at the same spanwise position as the boundary condition points given by equation (4). The spanwise station of the loading will be assumed to be at the middle of the segment, that is, at η_n. For symmetrical loading, the loading at wing center is constant in the range $-(1 - 3/4)/N \leq \eta \leq (1 - 3/4)/N$, and the middle of this segment is at $\eta_1 = 0$.

From equation (7) the loading at the n=N segment is

$$G_{\alpha NN} = \Delta G_{\alpha NN} = \frac{\pi}{3N} g_{NN}$$

At N-1 segment $$G_{\alpha N,N-1} = \Delta G_{\alpha NN} + \Delta G_{\alpha N,N-1} = \frac{\pi}{3N}(g_{NN} + g_{N,N-1})$$

Thus at the m segment $$G_{\alpha Nn} = \frac{\pi}{3N} \sum_{m=n}^{N} g_{Nm} \tag{20}$$

where g_{Nm} is given in equation (16) and in table 1, but with n=m numbers. These loadings are at the spanwise stations

$$\left.\begin{aligned} \eta_n &= \frac{n - 3/4}{N} \quad ; \text{ for } n > 1 \\ &= 0 \quad\quad\ ; \text{ for } n = 1 \end{aligned}\right\} \tag{21}$$

Comparable slender wing theory values of $G_\alpha(\eta_n)$ are given by equation (1) with η_n of equation (21). Comparison of equation (20) with the slender wing theory value of spanwise loading shows that the lattice-method loading requires a

factor. This spanwise loading factor is defined as

$$i_{Nn} = \frac{G_\alpha(\eta_n)\ \text{slender wing theory}}{G_\alpha(\eta_n)} \tag{22}$$

Numerical values of i_{Nm} computed from equation (22) are presented in table 3. These loading factors are very near to unity. Included are values for $N \to \infty$.

Lift-Curve Slope and Induced Drag

The lift coefficient is the integration of the loading coefficient, then

$$C_L = A \int_{-1}^{1} G(\eta)\, d\eta \tag{23}$$

Since ΔG_{Nn} is constant between η_{vn} and $-\eta_{vn}$, then the integration for lift is a summation of the pyramid layers of $2\eta_{vn}\,\Delta G_{Nn}$. Then by equation (23)

$$C_L = 2A \sum_{n=1}^{N} G_{Nn}\eta_{vn} \tag{24}$$

With the ΔG_{Nn} given in equation (7) and η_{vn} in equation (3), then equation (24) becomes C_{L_α}. The lift-curve slope is

$$C_{L_\alpha} = \frac{2\pi A}{3N^2} \sum_{n=1}^{N} (n - 1/4)g_{Nn} \tag{25}$$

where g_{Nn} is given in equation (16) and in table 1. With equation (16) inserted into (25) the lift-curve slope becomes $C_{L_\alpha} = \pi A/2$ for any value of N. This compares with the slender wing value given in equation (1).

In a following section for $N = \infty$ it is proven that $C_{L_\alpha} = \pi A/2$ for $N \to \infty$.

The induced drag coefficient is given by (for constant α_n)

$$C_{D_i} = \frac{A}{2} \int_{-1}^{1} \alpha_i G(\eta) d\eta = \frac{A}{2} \sum_{n=1}^{N} \alpha_n \Delta G_{Nn}\eta_{vn}$$

where α_n is that in equation (5) but with changed position of n and m. Since $\alpha_n = \alpha$ by the conditions of equation (6), and using equation (24), then $C_{D_i} = C_{L_\alpha}/2$. It was shown by equation (25) that $C_L = \pi A\alpha/2$ for any value of N, then

$$C_{D_i} = \frac{\pi A}{4} \alpha^2$$

which is then also valid for any value of N. This is identical to slender wing induced drag. Therefore, it is concluded that this lattice and boundary point distribution results in exact integrations for lift and induced drag for any interger N. This exactness was not unexpected since the mathematics is similar to the chordwise solution (ref. 20) in which the first harmonic solution (elliptic chord loading) integrates exactly.

Solutions for N Approaching Infinity

Detailed mathematical derivations are developed in reference 19. Here the results are a digest of the mathematics in that study. The primary purpose for exploring solutions at $N \to \infty$ is to prove that a finite lattice-method solution does mathematically converge to the exact solution. In this problem the exact solution is elliptical spanwise loading evaluated from slender wing theory. Mathematical proof is needed that the integration for lift remains exact as $N \to \infty$. Asymtotic values of the factors h_{Nn} and i_{Nn} as $N \to \infty$ are useful in the tables of these factors. As $N \to \infty$ the functions become so unique and manageable the reader will find a mathematical exciting experience.

Equation (16) can be used to mathematically prove that spanwise distribution predicted from finite element loading methods do converge on the exact answer as the number of elements are increased.

Using the relation for large factorials

$$N! \xrightarrow{N \to \infty} (2\pi)^{1/2} N^{N+1/2} e^{-N} \tag{26}$$

then equation (16) becomes (except at the point n=N, i.e. at $\eta=1$ when $N=\infty$)

$$g_{Nn} = \frac{3n\,(N+n)^{1/2}}{\pi(N+n)\,(N-n)^{1/2}} = \frac{3\frac{n}{N}}{\pi\left(1-\frac{n^2}{N^2}\right)^{1/2}} \tag{27}$$

Combining equations (3), (18), and (27) results in

$$G_\alpha{}'(\eta_{vn}) = \frac{-\eta_{vn}}{(1-\eta_{vn}{}^2)^{1/2}} \tag{28}$$

Equation (28) is the same as the loading gradient given in equation(1) by slender wing theory. Thus it is proven that as lattice panels are increased, the solution converges to the exact loading.

With the relation that

$$\frac{\Gamma(N + 1/2)}{\Gamma(N + 1)} \xrightarrow{N\to\infty} \frac{1}{(N + 1/4)^{1/2}} \tag{29}$$

then equation (17) can be expressed in the forms

$$\underset{\substack{n = \text{finite}}}{N\to\infty} \quad g_{N_N} = \frac{3n^2}{\pi N}\left[\frac{\Gamma(n + 1/2)}{\Gamma(n + 1)}\right]^2, \qquad \underset{\substack{N-n = \text{finite}}}{N\to\infty} \quad g_{N,N-n} = \frac{3N^{1/2}\,\Gamma(N - n + 1/2)}{\pi 2^{1/2}\,\Gamma(N - n + 1)} \tag{30}$$

Then for $N\to\infty$ the spanwise loading gradient factor of equation (19) becomes

$$\underset{\substack{n = \text{finite}}}{N\to\infty} \quad h_{Nn} = \frac{n - 1/4}{n}\left[\frac{\Gamma(n + 1)}{\Gamma(n + 1/2)}\right]^2, \qquad \underset{\substack{N-n = \text{finite}}}{N\to\infty} \quad h_{N,N-n} = \frac{\Gamma(N-n + 1)}{(N-n + 1/4)^{1/2}\Gamma(N-n + 1/2)} \tag{31}$$

With the use of the series summation

$$\sum_{p=0}^{N-m} \frac{\Gamma(p + 1/2)}{\Gamma(p + 1)} = 2(N - m + 1/2)\,\frac{\Gamma(N - m + 1/2)}{\Gamma(N - m + 1)} \tag{32}$$

the spanwise loading factor of equation (22) for $N\to\infty$ becomes

$$\underset{}{N=\infty} \quad i_{N,N-n} = \frac{(N - n + 3/4)^{1/2}\,\Gamma(N - n + 1)}{(N - n + 1/2)\,\Gamma(N - n + 1/2)} \tag{33}$$

Numerical values of equations (31) and (33) are listed in tables 2 and 3. Examination of these equations indicates simple relationships. These relationships extend to chordwise loading factors developed in a later section and can be expressed in one equation as follows:

for $N = N_c = \infty$

$$h_{N,N-n} = \frac{h_{Nn}^{1/2}}{(1-1/16n^2)^{1/2}} = \frac{i_{N,N-n+1}}{\left[1-1/16(N-n+1)^2\right]^{1/2}} = \frac{f_{N_c,N_c-n_c+1}}{\left[1-1/16(N_c-n_c-1)^2\right]^{1/2}} =$$

$$f_{N_c,n_c-1} \tag{34}$$

For the zero condition

$$h_{N,(N-n)=0} = f_{N_c,(n_c-1)=0} = \frac{2}{\pi^{1/2}} = 1.128379$$

For N-n = 1

$$h_{N,(N-n)=1} = f_{N_c,(n_c-1)=1} = \frac{4}{\sqrt{5\pi}} = 1.009253,\ h_{N,n=1} = .954930,\ i_{N,(N-n-+1)=1} =$$

$$f_{N_c,(N_c-n_c+1)=1} = .977205$$

For N = ∞ the expression for C_{L_α} develops into the following series summation:

$$C_{L_\alpha} = \left(\frac{A}{2}\right) 32\sqrt{2} \sum_{\Delta=0}^{\infty} \frac{(2\Delta)!}{2^{3\Delta}(\Delta!)^2(2\Delta+1)(2\Delta+3)(2\Delta+5)} \tag{35}$$

This factor of $A/2$ is π, thus $C_{L_\alpha} = \pi A/2$.

CHORDWISE VORTEX LATTICE

Formulation of Chordwise Lattice Matrix and Solution to Infinity

In reference 20 the lattice is distributed into equal length chord segments and the chord loading vortex is located at the 1/4 points of each of the chord segments; and boundary condition point at the 3/4 point of each of the chord segments. Then the load vortex chord station and the boundary condition chord station are respectively at

$$\xi_{m_c} = \frac{m_c-3/4}{N_c}\ ; \quad \xi_{m_e} = \frac{m_c-1/4}{N_c} \tag{36}$$

where $\xi = x/c$.

The loading equations to be solved are given as,

$$\sum_{n_e=1}^{N_c} \frac{e_{N_c n_c}}{2m_c-2n_c+1} = 1;\ m_c = 1, 2, \ldots N_c \tag{37}$$

where

$$e_{N_c n_c} = \frac{N_c \Gamma_{n_c}}{\pi c V \alpha} = \frac{\gamma_{n_c}}{\pi V \alpha} = \frac{-\Delta C_{pn_c}}{2\pi\alpha} \tag{38}$$

The matrix inversion of equation (37) is obtained as a factorial function

$$e_{N_c n_c} = \frac{(2N_c-2n_c+1)_{odd!}\ (2n_c-3)_{odd!}}{(2N_c-2n_c)_{ev!}\ (2N_c-2)_{ev!}} = \frac{(2N_c-2n_c+1)!\ (2n_c-2)!}{2^{2N_c-2}\left[(N_c-n_c)!(n_c-1)!\right]^2} \qquad (39)$$

In terms of Gamma functions

$$e_{N_c n_c} = \frac{2n_c(2N_c-2n_c+1)\ \Gamma(n_c+1/2)\ \Gamma(N_c-n_c+1/2)}{\pi(2n_c-1)\ \Gamma(n_c+1)\ \Gamma(N_c-n_c+1)}$$

Numerical values of equation (39) are presented in table 4.

Chordwise Loading Factor

The exact solution by thin wing theory gives the additional loading by the function [using ξ_{m_c} defined in eq. (36)]

$$e_{N_c n_c} = \frac{\gamma_{n_c}}{\pi V\alpha} = \frac{2}{\pi}\left(\frac{1-\xi_{m_c}}{\xi_{m_c}}\right)^{1/2} = \frac{2}{\pi}\left(\frac{N_c}{n_c-3/4}-1\right)^{1/2} \qquad (40)$$

The chordwise loading factor is defined by the ratio of equation (40) to equation (39).

(41)

$$f_{N_c n_c} = \frac{e_{N_c n_c thin}}{e_{N_c n_c}} = \frac{\gamma_{n_c thin}}{\gamma_{n_c}} = \frac{(N_c-n_c+3/4)^{1/2}\ (2n_c-1)\ \Gamma(n_c+1)\ \Gamma(N_c-n_c+1)}{n_c(2N_c-2n_c+1)\ (n_c-3/4)^{1/2}\ \Gamma(n_c+1/2)\ \Gamma(N_c-n_c+1/2)}$$

Numerical evaluation of equation (41) for a range of N_c are given in table 5.

Chordwise Lift-Curve Slope and Pitching Moment

Section wing lift is the integration of the chordwise loading and section moment is the integration of the product of chordwise loading and moment arm. In mathematical representation

$$c_\ell = 2\int_0^1 \frac{\gamma}{Vc}\, d\xi \quad , \qquad c_{m_{LE}} = 2\int_0^1 \frac{\gamma}{Vc}\, \xi d\xi \qquad (42)$$

The lattice loading is constant with ξ over the interval

$\Delta\xi_{n_c} = [n_c-(n_c-1)]/N_c = 1/N_c$ and the lattice load vortex is located at

$\xi_{n_c} = (n_c-3/4)/N_c$ along the chord and the moment arm extends to this vortex.

Then with equation (38) equation (42) becomes

$$c_{\ell_\alpha} = \frac{2\pi}{N_c} \sum_{n_c=1}^{N_c} e_{N_c n_c} \quad , \qquad c_{m_{\alpha_{LE}}} = \frac{2\pi}{N_c^2} \sum_{n_c=1}^{N_c} (n_c - 3/4)\, e_{N_c n_c} \tag{43}$$

The summation terms in equation (43) are listed in table 4 which when inserted into equation (43) show that the lift and moment for arbitrary N_c is the same as predicted by thin wing theory, that is

$$c_{\ell_\alpha} = 2\pi, \quad c_{m_{\alpha_{LE}}} = \frac{\pi}{2}, \quad \text{a.c.} = \frac{c_{m_{\alpha_{LE}}}}{c_{\ell_\alpha}} = 1/4 \tag{44}$$

Proof that c_{ℓ_α} is Exact at All Values of N

Inserting equation (39) into (43) results in

$$c_{\ell_\alpha} = \frac{4}{N_c} \sum_{n_c=1}^{N_c} \frac{n_c(2N_c - 2n_c + 1)\, \Gamma(n_c + 1/2)\, \Gamma(N_c - n_c + 1/2)}{(2n_c - 1)\, \Gamma(n_c + 1)\, \Gamma(N_c - n_c + 1)} \tag{45}$$

Now $\Gamma(n+1/2) = (n-1/2)\,\Gamma(n-1/2)$; $\Gamma(N-n-1/2) = \Gamma(N-n+1/2)/(N-n-1/2)$; and $\Gamma(n+1) = n\Gamma(n) = n!$, then

$$c_{\ell_\alpha} = 4 \sum_{n_c=0}^{N_c-1} \frac{N_c - n_c}{N_c} \frac{\Gamma(n_c + 1/2)\, \Gamma(N_c - n_c + 1/2)}{n_c!\, (N_c - n_c)!} \tag{46}$$

The Gamma functions and factorials in equation (46) show that this product term is a symmetric function which is factored by an antisymmetric term $(N_c - n_c)/N_c$. Then some of the high n_c terms cancel the low n_c terms. By expanding the summation a new summation can be formed given by

$$c_{\ell_\alpha} = 2\pi \sum_{n_c=0}^{n_c \le \frac{N_c}{2}} \frac{\varepsilon\left(\frac{N_c}{2} - n_c\right)}{\pi} \frac{\Gamma(n_c + 1/2)\, \Gamma(N_c - n_c + 1/2)}{n_c!\, (N_c - n_c)!} \tag{47}$$

where

$$\epsilon\left(\frac{N_c}{2} - n_c\right) = 1 \text{ for } n_c = \frac{N_c}{2}, = 2 \text{ for } n_c \neq \frac{N_c}{2}$$

The summation term in equation (47) is the Legendre polynomial of the first kind $P_{N_c}(\cos\theta)_{\theta=0}$ (see p. 36, ref. 24) and $P_{N_c}(1) = 1$ for any N_c. Thus the lift-curve slope is 2π for any N_c which is that predicted by thin wing theory.

Chordwise Solutions for $N \to \infty$

For $N_c \to \infty$ and n_c finite or $N_c - n_c$ finite then equation (39) becomes

$$\left.\begin{aligned} &\substack{N_c \to \infty \\ n_c = \text{finite}} \\ &e_{N_c n_c} = \frac{4 N_c^{1/2} n_c \, \Gamma(n_c + 1/2)}{\pi(2n_c - 1)\,\Gamma(n_c + 1)} \\ &\substack{N_c \to \infty \\ N_c - n_c = \text{finite}} \\ &e_{N_c, N_c - n_c} = \frac{2(N_c - n_c + 1/2)\,\Gamma(N_c - n_c + 1/2)}{\pi n_c^{1/2}\,\Gamma(N_c - n_c + 1)} \end{aligned}\right\} \quad (48)$$

For both N_c and n_c large [using eq. (29)], equation (39) becomes

$$\substack{N \to \infty \\ n_c \to \infty}$$

$$e_{N_c n_c} = \frac{2(N_c - n_c)^{1/2}}{\pi n_c^{1/2}} = \frac{2}{\pi}\left(\frac{1-\xi}{\xi}\right)^{1/2} \quad (49)$$

Equation (49) is identical to the thin wing theory additional loading given in equation (40) and shows that a chord lattice solution converges to mathematical exactness as the lattice grid becomes infinite. With equations (48), (40), and (41) the chordwise loading factor at wing leading edge is given by (for $N_c \to \infty$)

$$f_{N_c n_c} = \frac{\Gamma(n_c - 1 + 1)}{(n_c - 1 + 1/4)^{1/2}\,\Gamma(n_c - 1 + 1/2)} \quad (50)$$

This function is identical to that of equation (31) when $n_c - 1 = N - n$, and is listed in equation (34). With equations (48), (40), and (41), the chordwise

loading factor at wing trailing edge is given by (for $N_c \to \infty$)

$$f_{N_c,N_c-n_c} = \frac{(N_c-n_c+3/4)^{1/2}\ \Gamma(N_c-n_c+1)}{(N_c-n_c+1/2)\ \Gamma(N_c-n_c+1/2)} \tag{51}$$

This function is identical to $i_{N,N-n}$ of equation (33) when $N_c-n_c = N-n$, and is listed in equation (34).

A_e-VORTEX LATTICE

Dependency of Spanwise Lattice on Effect of Aspect Ratio

As aspect ratio approaches zero the spanwise optimum lattice arrangement is that defined by equation (3), that is at $\eta_{vn} = (n-1/4)/N$. As aspect ratio approaches infinity the spanwise lattice arrangement is the planform lattice which positions the trailing vortices at $\eta_{vn} = n/N$, that is at the outside edge of the lattice panel including a vortex at the wingtip. This is because at $A = \infty$ the spanwise loading has the same distribution as the wing chord along the span. This high loading near the wing tip (when $A = \infty$) must be taken into account by the lattice trailing vortices. The objective here is to develop an aspect ratio function factor for the lateral panel positions which asymptotically approaches the correct values at $A_e \to 0$ and at $A_e \to \infty$. The subscript e denotes the effective swept panel aspect ratio given by

$$A_e = A/\cos\Lambda_{1/2} \tag{52}$$

The planform lattice ($\eta_{vn} = n/N$) is the lateral lattice arrangement that has been in general use in most vortex-lattice methods.

An aspect ratio equal to four is about an aerodynamic mean between $0 \le A_e \le \infty$. Loading values based on the $A_e \to 0$ lattice and on the $A_e \to \infty$ lattice will be computed for an $A_e = 4$ rectangular wing. Comparison with the loading predicted by an accurate analysis will establish the A-effect function that is needed. By Biot-Savart law the downwash due to an unskewed horseshoe vortex is

$$\left(\frac{w}{V}\right)_{m,m_c} = \frac{G_{nn_c}}{2\pi\xi_0}\left[\frac{\xi_0 + \sqrt{\xi_0^2+(\eta_{wm}-\eta_{\Delta n}+\eta_{vn})^2}}{\eta_{wm}-\eta_{\Delta n}+\eta_{vn}} - \frac{\xi_0 + \sqrt{\xi_0^2+(\eta_{wm}-\eta_{\Delta n}-\eta_{vn})^2}}{\eta_{wm}-\eta_{\Delta n}-\eta_{vn}}\right] \tag{53}$$

Where $\xi_0 = \xi_{wm_c} - \xi_{vn_c}$, and G_{nn_c} is the dimensionless vortex strength of the elemental horseshoe vortex. For $N_c = 1$ solution, ξ_0 remains constant equal to 1/4 for $A = 4$. $\eta_{\Delta n}$ is the lateral middle of the n panel. For the slender wing ($A_e \to 0$) lattice use

$$\eta_{vn} = \frac{n-1/4}{N} \quad , \quad \eta_{wm} = \frac{m-3/4}{N} \quad , \quad \eta_{\Delta n} = 0 \tag{54}$$

For the planform lattice use

$$\eta_{vn} = \frac{n}{N} \quad , \quad \eta_{wm} = \frac{m-1/2}{N} \quad , \quad \eta_{\Delta n} = 0 \tag{55}$$

The equation to be solved for additional loading for an $N_c = 1$ solution, A = 4 rectangular wing is

$$1 = \frac{2}{3N} \sum_{n=1}^{N} g_{Nn} \left[\frac{1/4+\sqrt{1/16+(\eta_{wm}+\eta_{vn})^2}}{\eta_{wm}+\eta_{vn}} - \frac{1/4+\sqrt{1/16+(\eta_{wm}-\eta_{vn})^2}}{\eta_{wm}-\eta_{vm}} \right] \tag{56}$$

Wing lift-curve slope is determined from equation (24) and wing loading by equation (20) with which

$$\frac{(c_\ell c)_n}{C_L c_{av}} = \frac{2A}{C_{L_\alpha}} \, i_{Nn} G_{\alpha_{Nn}} \tag{57}$$

where for the A→0 lattice i_{Nn} values are given in table 3, while for the planform lattice i_{Nn} are all unity. Results of the solutions of equation (56) with the $A_e \to 0$ lattice of (54) and with the planform lattice of (55), for increasing N, are presented in tables 6 and 7. An accurate loading prediction of this A = 4 rectangular wing is made in reference 19. From reference 19

$$\left.\begin{aligned} C_{L_\alpha} &= 3.6623, \ \eta = \cos\phi \\ \frac{c_\ell}{C_L} &= \frac{4}{\pi}(\sin\phi + .07879\sin 3\phi + .01290\sin 5\phi + .00350\sin 7\phi + .00170\sin 9\phi) \end{aligned}\right\} \tag{58}$$

Percent differences from the values of equation (58) are shown in tables 6 and 7. For this A = 4 wing the A→0 lattice has less than one-half the error of the planform lattice.

Spanwise A_e-Vortex Lattice

Since for the A = 4 wing the A→0 lattice prediction is too small and the planform (A→∞) lattice prediction too large then a factor can be developed between the two which forms the basis of spanwise A_e-lattice arrangement. This factor is $2/\sqrt{A_e+4}$, then for the A_e-lattice

$$\left.\begin{aligned} \eta_{vn} &= \frac{1}{N}\left(n-\frac{1}{2\sqrt{A_e+4}}\right)\ ,\ \eta_{wm}=\frac{1}{N}\left(m-\frac{1}{2}-\frac{1}{2\sqrt{A_e+4}}\right) \\ i_{ANn} &= 1-(1-i_{Nn})\frac{2}{\sqrt{A_e+4}}\ ,\ \eta_1=\frac{1}{N}\left(\frac{1}{2}-\frac{1}{\sqrt{A+4}}\right)\ ,\ \eta_n=\frac{1}{N}\left(n-\frac{1}{2}-\frac{1}{2\sqrt{A_e+4}}\right) \end{aligned}\right\} \quad (59)$$

where A_e is defined in equation (52) and η_n is the spanwise position of the computed loading distribution. These spanwise lattice panel positions asymptotically approach the A→0 lattice and the planform lattice as A→0 and ∞ respectively. With equation (59) the solutions of equation (56) for lift and loading are listed in tables 6 and 7. With the A_e-lattice the predicted lift and loading is accurate for all N's which was the basis for the term optimum applied to the A→0 lattice and chordwise lattice. Equation (59) is simply a mathematical statement that relative to the planform lattice all the panels are shifted inboard by $1/2N\sqrt{A_e+4}$, and that the downwash point is at the lateral center of each panel except in the wing root panel.

Application of the A_e-Vortex Lattice

For a uniform vortex lattice, the elemental skewed horseshoe vortex lateral position at the trailing vortices is given by η_{vn} in equation (59) and the chordwise position by ξ_{vnc} in equation (36). The downwash points are positioned laterally at η_{wm} in equation (59) and chordwise at ξ_{wmc} in equation (36). Let Γ_{nnc} be the unknown circulation strength of the elemental skewed horseshoe vortex. For symmetric wing loading Γ_{nnc} is determined from an NN_C matrix solution which satisfies NN_C downwash point boundary conditions. The pressure coefficient at span station η_n in equation (59) and chord station $\xi_{vnc} = (n_c-3/4)/N_C$ is given by

$$\Delta C_{p_{nn_c}} = -2N_c i_{ANn} f_{N_c n_c} \frac{\Gamma_{nn_c}}{c_n V} \quad (60)$$

where spanwise and chordwise loading factors are included [eq. (59), tables 3 and 5]. Now

$$\Gamma_n = \sum_{n_c=1}^{N_c} \Gamma_{nn_c} \quad (61)$$

then the spanwise loading at η_n of equation (59) is

$$\Gamma_n\Big)_{at\eta_n} = \frac{V}{2}c_\ell c\Big)_{at\eta_n} = i_{ANn}\Gamma_n \tag{62}$$

which includes the spanwise loading factor [eq. (59), table 3]. The spanwise loading gradient at span station η_{vn} in equation (59) is

$$\frac{d\Gamma_n}{d\eta} = -h_{ANn}\, N(\Gamma_n - \Gamma_{n+1}) \tag{63}$$

where Γ_n is given in equation (61) and where the spanwise loading gradient factor is given by

$$h_{ANn} = 1-(1-h_{Nn})\frac{2}{\sqrt{A_e+4}}\text{ , with } h_{Nn} \text{ in table 2.}$$

The lift coefficient is [Γ_n from eq. (61)]

$$C_L = \frac{2A}{NbV}\left(\frac{3}{4}\Gamma_1 + \sum_{n=2}^{N}\Gamma_n\right) \tag{64}$$

The induced drag is given by

$$\left.\begin{aligned} C_{D_i} &= \frac{A}{2bV}\int_{-1}^{1}\alpha_i\Gamma d\eta = \frac{A}{NbV}\left(\frac{3}{4}\alpha_1\Gamma_1 + \sum_{n=2}^{N}\alpha_n\Gamma_n\right) \\ \alpha_n &= \frac{N}{\pi bV}\left[\left(\frac{1}{N-n+1/2}+\frac{1}{N+n-1}\right)\Gamma_N + \sum_{m=1}^{N-1}\left(\frac{1}{m-n+1/2}+\frac{1}{m+n+1}\right)(\Gamma_m-\Gamma_{m+1})\right] \end{aligned}\right\} \tag{65}$$

where Γ_n is given in equation (61). For spanwise loading distribution already known then equation (65) provides a convenient method for predicting induced drag. For this case $\Gamma_n)_{at\eta_n}$ is known then Γ_n is determined from equation (62) for application in (65).

CONCLUDING REMARKS

The application of the vortex-lattice method to the slender wing configuration has provided a rigorous analytical basis for the spanwise properties of the vortex-lattice method. Mathematical similarities are shown between the spanwise panel lattice solution and the chordwise solution which converge to thin wing theory results. As the number of chordwise panels approaches infinity, thin wing theory chordwise loading is predicted exactly except in the limit points exactly at the leading edge and at the trailing edge. At

these two points chordwise loading factors are mathematically evaluated which are useful in finite panel solutions. Similarly, as the number of spanwise panels becomes infinite, slender wing theory spanwise loading is predicted exactly except at the point of the wing tip. At this point a spanwise loading factor is mathematically determined from a limit solution. The presentation in this paper is based on a planform uniform distribution of panels chordwise and spanwise. In a discussion in 1972 Mr. W. B. Kemp, Jr. of NASA-Langley said he had found that the chordwise vortex-lattice solution gave an accurate integrated lift for an arbitrary planform panel distribution along the chord. As part of the present work this was investigated and it was shown that using the 1/4 - 3/4 rule for locating the vortex and downwash point in the planform panel, the chordwise lift-curve slope of 2π and also the spanwise slender wing value of $\pi A/2$ are predicted for any distribution of planform panels on the wing and for any total number of panels. However, the loading distribution factors are not as near unity. The aspect ratio effect on spanwise lattice arrangement has a weak chordwise counterpart for a chordwise lattice arrangement. An initial study of this effect indicates that the chordwise lattice arrangement differs when aspect ratio is less than unity. In conclusion, the A_e-vortex-lattice arrangement of the previous section provides a uniform uncomplicated, accurate system. It leads to computations with a high accuracy to work ratio.

REFERENCES

1. Falkner, V. M.: The Calculation of Aerodynamic Loading on Surfaces of Any Shape. A.R.C.R. & M. 1910, Aug. 1943, Aeronautical Research Council, England.

2. VanDorn, N. H.: and DeYoung, J.: A Comparison of Three Theoretical Methods of Calculating Span Load Distribution on Swept Wings. NASA TN 1491, 1947.

3. Runyan, H. L. and Woolston, D. C.: Method for Calculating the Aerodynamic Loading on an Oscillating Finite Wing in Subsonic and Sonic Flow. TR1322, 1957. NACA.

4. Rubbert, P. E.: Theoretical Characteristics of Arbitrary Wings by a Nonplanar Vortex Lattice Method. Report D6-9244, The Boeing Co., Seattle, Washington, 1964.

5. Dulmovits, J.: A lifting Surface Method for Calculating Load Distributions and the Aerodynamic Influence Coefficient Matrix for Wings in Subsonic Flow. Report ADR 01-02-64.1, 1964, Grumman Aerospace Corp., Bethpage, N.Y.

6. Hedman, S. G.: Vortex Lattice Method for Calculation of Quasi Steady State Loadings on Thin Elastic Wings In Subsonic Flow. Report 105, Oct. 1965. Aeronautical Research Institute of Sweden.

7. Belotserkovskii, S. M.: The Theory of Thin Wings in Subsonic Flow. Plenum Press, New York 1967.

8. Landahl, M. T. and Stark, V.J.E.: Numerical Lifting-Surface Theory-Problems and Progress. AIAA J., Vol. 6, No. 11, Nov. 1968, pp 2049-2060.

9. Woodward, F. A.: Analysis and Design of Wing-Body Combinations at Subsonic and Supersonic Speeds. J. of Aircraft, Vol. 5,No. 6, Nov.-Dec. 1968, pp. 528-534.

10. Albano E., and Rodden, W. P.: A Doublet-Lattice Method for Calculating Lift Distributions on Oscillating Surfaces in Subsonic Flow. AIAA J., Vol. 7, No.2, Feb. 1969, pp 279-285.

11. James, R. M.: On the Remarkable Accuracy of the Vortex Lattice Discretization in Thin Wing Theory. Report DAC-67211, Feb 1969, McDonnell Douglas Corp., Long Beach, California.

12. Houbolt, J. C.: Some New Concepts in Oscillatory Lifting Surface Theory. Report AFFDL-TR-69-2, June 1969, U. S. Air Force Flight Dynamics

Laboratory, Wright-Patterson Air Force Base, Ohio.

13. Margason, R. J. and Lamar, J. E.: Vortex-Lattice Fortran Program for Estimating Subsonic Aerodynamic Characteristics of Complex Planforms. NASA TN D-6142, Feb. 1971, 139 pp.

14. Kalman, T. P., Rodden, W. P., and Giesing, J. P.: Application of the Doublet-Lattice Method to Nonplanar Configurations in Subsonic Flow. J. of Aircraft, Vol 8, No. 6, June 1971, pp 406-413.

15. Lamar, J. E.: Nonplanar Method for Predicting Incompressible Aerodynamic Coefficients of Rectangular Wings with Circular-Arc Camber. Ph.D. Dissertation, Aerospace Engineering, Virginia Polytechnic Institute and State University, December 1971, 91 pp.

16. Seath, D. D. and DeYoung, J.: Generation of Finite-Difference Mesh Geometry Configurations. Convair Report ERR-FW-1240, Dec. 1971. General Dynamics, Fort Worth, Texas, 80 pp.

17. DeYoung, J. and Seath, D. D.: Examination of Mesh Geometry Generation Techniques. UTA Report No. AE 72-01, Dec 1971, University of Texas at Arlington, Arlington, Texas, 18 pp.

18. Lan, C. E.: A Quasi-Vortex-Lattice Method in Thin Wing Theory. J. of Aircraft, Vol. 11, No. 9, Sept. 1974, pp 518-527.

19. DeYoung, J.: Wing Loading Theory Satisfying All Boundary Points. Ph.D. Dissertation, The University of Texas at Arlington, Arlington, Texas, Dec. 1975, 180 pp.

20. DeYoung J.: Convergence-Proof of Discrete-Panel Wing Loading Theories. J. of Aircraft, Vol. 8, No.10, Oct. 1971, pp. 837-838.

21. Jones, R. T.: Properties of Low-Aspect Ratio Pointed Wings at Speeds Below and Above the Speed of Sound. NACA Report 835, 1946.

22. DeYoung, J.: Spanwise Loading for Wings and Control Surfaces of Low Aspect Ratio, NASA TN 2011, Jan. 1950, 36 pp.

23. Handbook of Mathematical Functions with Formulas, Graphs, and Mathematical Tables. Edited by Abramowitz, M. and Stegun, I.A., National Bureau of Standards, Applied Mathematics Series 55, U.S. Government Printing Office, 1965, 1046 pp.

24. Mangulis, V.: Handbook of Series for Scientists and Engineers. Academic Press. New York and London, 1965, 134 pp.

TABLE 1. - g_{Nn}, SPANWISE SOLUTIONS OF EQUATION (6)

N \ n	1	2	3	4	5	6
1	1					
2	$\frac{2x3}{3x5}$	$\frac{2x3^4}{3x5x7}$				
3	$\frac{3^3}{3x5x7}$	$\frac{2^3x3^4}{3x5x7x9}$	$\frac{2x3^4x5^3}{11_{odd}!}$			
4	$\frac{2^2x3^2x5}{3x5x7x9}$	$\frac{2^2x3^5x5}{11_{odd}!}$	$\frac{2^2x3^5x5^3}{13_{odd}!}$	$\frac{2^2x3^3x5^3x7^3}{15_{odd}!}$		
5	$\frac{3^2x5^2x7}{11_{odd}!}$	$\frac{2^3x3^5x5^2}{13_{odd}!}$	$\frac{2x3^6x5^3x7}{15_{odd}!}$	$\frac{2^5x3^3x5^3x7^3}{17_{odd}!}$	$\frac{2x3^3x5^3x7^3x9^3}{19_{odd}!}$	
6	$\frac{2x3^5x5x7}{13_{odd}!}$	$\frac{2x3^5x5^2x7^2}{15_{odd}!}$	$\frac{2^4x3^5x5^4x7}{17_{odd}!}$	$\frac{2^4x3^6x5^3x7^3}{19_{odd}!}$	$\frac{2^2x3^9x5^4x7^3}{21_{odd}!}$	$\frac{2^2x3^9x5^2x7^3x11^3}{23_{odd}!}$
N	$\frac{3N(2N-3)_{odd}!}{(2N+1)_{odd}!} = \frac{3N}{4N^2-1}$					$\frac{3x2^{N-1}[(2N-1)_{odd}!]^3}{(N-1)!(4N-1)_{odd}!}$

TABLE 2. - h_{Nn}, SPANWISE LOADING GRADIENT FACTOR

N \ n	1	2	3	4	5	6
1	1.082788					
2	.965721	1.118660				
3	.958851	1.000148	1.124345			
4	.956981	.993739	1.005515	1.126193		
5	.956199	.992082	.999207	1.007242	1.127013	
6	.955795	.991404	.997613	1.000965	1.008002	1.127446
∞	.954930	.990297	.995956	.997804	.998625	.999060
∞	1.000564	1.000858	1.001459	1.003004	1.009253	1.128379

TABLE 3. - i_{Nn}, SPANWISE LOADING FACTOR

N \ n	1	2	3	4	5	6
	$\eta=0$					
1	.954930					
2	.983016	.966313				
3	.990965	.988798	.972705			
4	.994332	.993811	.992034	.974770		
5	.996085	.995935	.995712	.993301	.975684	
6	.997119	.997082	.997167	.996548	.993923	.976166
$-N+n+6$						
∞	.999530	.999312	.998901	.997976	.995137	.977205

TABLE 4. - $e_{N_c n_c}$, CHORDWISE SOLUTIONS OF EQUATION (37)

N_c \ n_c	1	2	3	4	5	6	$\sum_{n_c=1}^{N_c} e_{N_c n_c}$	$\sum_{n_c=1}^{N_c} (n_c-\frac{3}{4}) e_{N_c n_c}$
1	1						1	1/4
2	3/2	1/2					2	4/4
3	15/8	3/4	3/8				3	9/4
4	35/16	15/16	9/16	5/16			4	16/4
5	315/128	35/32	45/64	15/32	35/128		5	25/4
6	693/256	315/256	105/128	75/128	105/256	63/256	6	36/4
							II	II
							N	$N^2/4$

TABLE 5. - $f_{N_c n_c}$, CHORDWISE LOADING FACTOR

N_c \ n_c	1	2	3	4	5	6
1	1.102658					
2	1.122892	.986247				
3	1.126095	1.004345	.980140			
4	1.127139	1.007210	.998126	.978631		
5	1.127603	1.008144	1.000974	.996589	.978043	
6	1.127848	1.008559	1.001902	.999433	.995991	.977756
∞	1.128379	1.009253	1.003004	1.001459	1.000858	1.000564
∞	.999530	.999312	.998901	.997976	.995137	.977205

TABLE 6. - LATTICE COMPARISONS FOR PREDICTING C_{L_α}, A=4 RECTANGULAR WING

N	planform lattice		A→0 lattice		A_e-lattice	
	C_{L_α}	ΔC_{L_α},%	C_{L_α}	ΔC_{L_α},%	C_{L_α}	ΔC_{L_α},%
1	4.4904	22.61	3.2513	-11.22	3.6176	-1.22
2	4.1267	12.68	3.4914	- 4.67	3.6787	.45
3	3.9629	8.21	3.5367	- 3.43	3.6622	0

TABLE 7. - LATTICE COMPARISONS FOR PREDICTING $\frac{c_\ell}{C_L}$, A= 4 RECTANGULAR WING

N	planform lattice				A→0 lattice				A_e-lattice				
	n	$\frac{c_\ell}{C_L}$	$\frac{c_\ell}{C_{L,19}}$	$\Delta\frac{c_\ell}{C_L}$,%	n	$\frac{c_\ell}{C_L}$	$\frac{c_\ell}{C_{L,19}}$	$\Delta\frac{c_\ell}{C_L}$,%	n	$\frac{c_\ell}{C_L}$	$\frac{c_\ell}{C_{L,19}}$	$\Delta\frac{c_\ell}{C_L}$,%	i_{ANn}
1	.500	1	1.092	-8.45	0	1.273	1.187	7.25	.146	1.176	1.179	-. 29	.9681
2	.250	1.088	1.165	-6.62	0	1.230	1.187	3.65	.073	1.185	1.185	0	.9880
	.750	.912	.914	- .21	.625	1.026	1.024	.19	.662	.989	.995	- .67	.9762
3	.167	1.126	1.177	-4.33	0	1.224	1.187	3.09	.049	1.194	1.187	.58	.9936
	.500	1.049	1.092	-4.01	.417	1.145	1.124	1.87	.441	1.115	1.115	- .04	.9921
	.833	.826	.799	3.34	.750	.891	.914	-2.57	.77[illegible]	.871	.883	-1.36	.9807

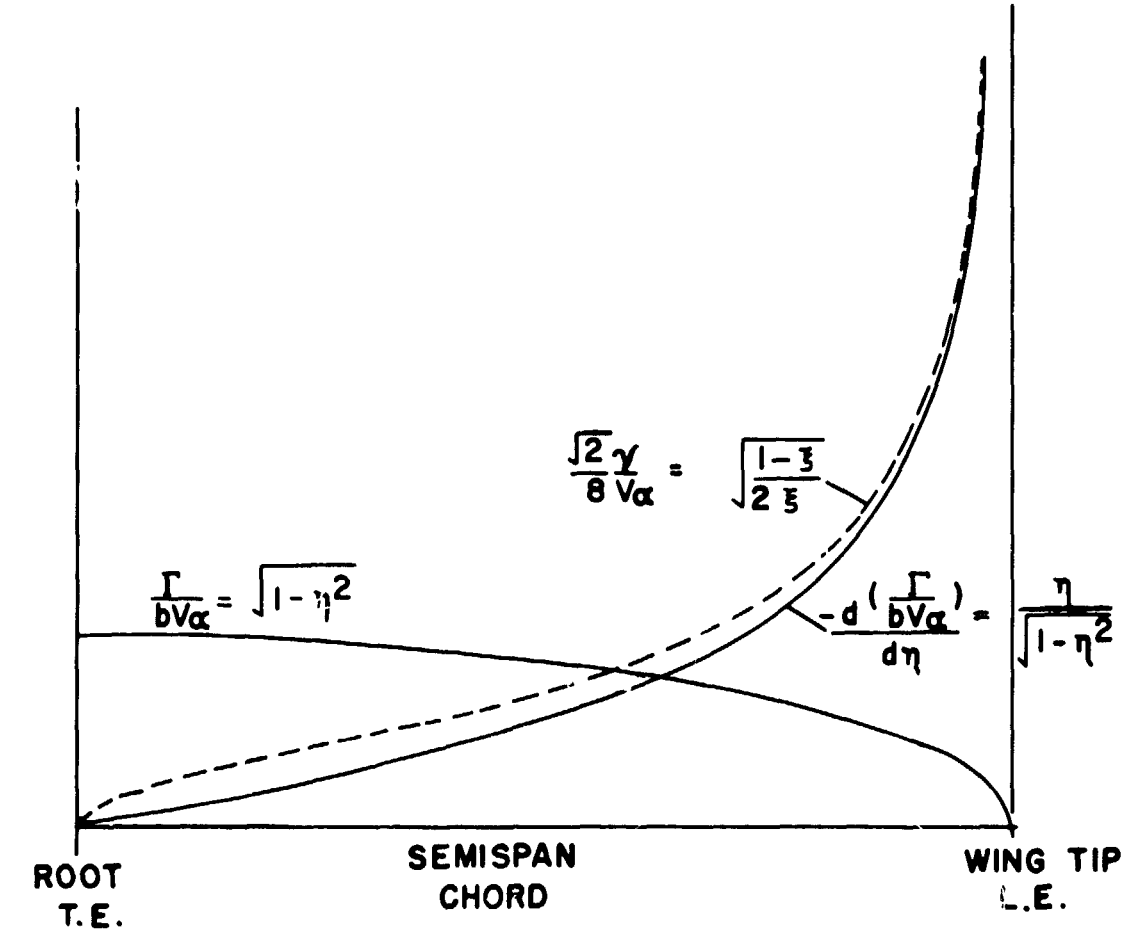

Figure 1.- Comparison of chordwise loading with spanwise loading gradient.

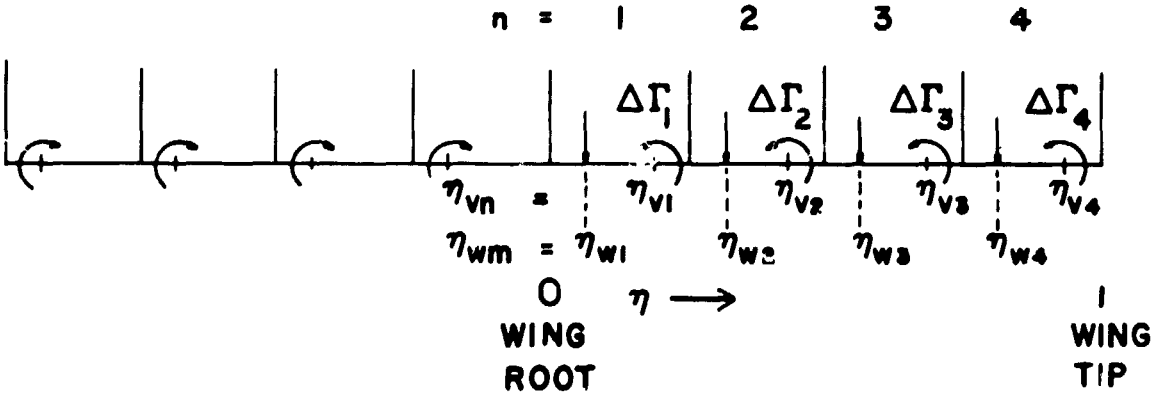

Figure 2.- Spanwise panel distribution for N = 4, and location of trailing vortex of 1/4 panel width in from wing tip, and location of boundary point at 3/4 panel width in from wing tip.